ELSEVIER

Available online at www.sciencedirect.com

SCIENCE DIRECT®

Polymer 46 (2005) 8340–8354

polymer

www.elsevier.com/locate/polymer

Estimation of intrinsic rate coefficients in vinyl chloride suspension polymerization

T. De Roo, J. Wieme, G.J. Heynderickx, G.B. Marin*

Laboratorium voor Petrochemische Techniek, Ghent University, Krijgslaan 281-(S5), B-9000 Ghent, Belgium

Received 15 April 2005; received in revised form 24 June 2005; accepted 24 June 2005
Available online 21 July 2005

Abstract

The pre-exponential factor and the activation energy of the intrinsic rate coefficients for propagation, chain transfer to monomer, chain initiation by a Cl radical and termination in the suspension polymerization of vinyl chloride are estimated by regression of experimental data for the monomer conversion, ranging from 3 to 85%, and for the moments of the molecular mass distribution as a function of batch time over the temperature range of 308–338 K and for initiator (*tert*-butyl peroxyneodecanoate) concentrations from 0.026 to 3.0 wt%, based on the monomer. Termination by combination is the dominant termination mechanism. Cl radicals, formed in the chain transfer to monomer, contribute to the termination by recombination with macroradicals and, hence, attenuate the gel effect. Physically meaningful and statistically significant estimates for the pre-exponential factors and activation energies, 24.9 kJ mol^{-1} for propagation and 54.3 kJ mol^{-1} for chain transfer, allow to describe the experimental data over the full range of investigated conditions.

Keywords: Parameter estimation; Poly(vinyl chloride); Intrinsic kinetics

1. Introduction

The vinyl chloride suspension polymerization has been modeled by several groups, most recently by those of Xie et al. [1,2], Kiparissides et al. [3], Talamini et al. [4,5] and Krallis et al. [6]. The derived models allow to calculate among others, the monomer conversion and the moments of the molecular mass distribution (MMD) as a function of polymerization time. In the model of Xie et al. [1,2] and of Talamini et al. [4,5] diffusion parameters are estimated from a set of experimental data to enable the calculation of diffusional limitations on the polymerization reactions. In the model of Kiparissides et al. [3] diffusional limitations are accounted for by implementing free volume theory to calculate the diffusion coefficients and adjusting some of the diffusion parameters to experimental data. All of these authors use values for the important intrinsic rate coefficients of the polymerization reactions (propagation, chain transfer, termination) obtained from literature [7,8] and corresponding to other than vinyl chloride suspension polymerization systems. The kinetic data from Burnett and Wright [7] are related to photosensitized solution polymerization, while those from Abdel-Alim and Hamielec [8] originate from bulk polymerization experiments. Recent literature [9–11] provides no values for the vinyl chloride polymerization either.

The estimation of intrinsic rate coefficients of free-radical polymerization reactions by regression of experimental data is virtually impossible without considering the effects of different diffusion phenomena [12,13]. The three main reactions that can become diffusion-controlled are initiation, propagation and termination, corresponding to the so-called cage, glass, and gel effect. Accounting for diffusion phenomena during the regression is necessary to obtain information on intrinsic rate coefficients because experimental data almost inevitably are affected by diffusion. Hence, the diffusion parameters and intrinsic rate coefficients are often estimated simultaneously by regression of experimentally obtained monomer conversions and moments of the MMD [14,15]. Such an approach can lead to strongly correlated values of the estimated parameters. It has been shown, however, that for vinyl chloride suspension polymerization, the diffusion can be

---

* Corresponding author. Tel.: +32 9 264 4516; fax: +32 9 264 4999.
E-mail address: guy.marin@ugent.be (G.B. Marin).

0032-3861/$ - see front matter © 2005 Published by Elsevier Ltd.
doi:10.1016/j.polymer.2005.06.091

Nomenclature

a	root-mean-square end-to-end distance per square root of the number of monomer units in a polymer chain [m]
A^*	reparameterized pre-exponential factor of intrinsic rate coefficient [$m^3\ mol^{-1}\ s^{-1}$]
Cl_k	concentration of Cl radicals in phase k [$mol\ m^{-3}$]
D_x	self-diffusion coefficient of component x (x = Cl, i, m) [$m^2\ s^{-1}$]
$D_{x,0}$	pre-exponential factor of the self-diffusion coefficient of component x (x = Cl, i, m) [$m^2\ s^{-1}$]
$D_x(cent)$	centre-of-mass diffusion coefficient of a component x (x = Cl, i, m) [$m^2\ s^{-1}$]
D_p^i	centre-of-mass diffusion coefficient of a macroradical with chain length i [$m^2\ s^{-1}$]
$D_p(rd)$	reaction diffusion coefficient [$m^2\ s^{-1}$]
D_{p+rd}^i	diffusion coefficient of a macroradical with chain length i [$m^2\ s^{-1}$]
$\bar{D}_{p,0}$	pre-exponential factor of the macroradical self-diffusion coefficient including the activation energy [$m^2\ s^{-1}$]
$D_{reptation}^i$	reptation theory polymer melt diffusion coefficient [$m^2\ s^{-1}$]
E	activation energy [$J\ mol^{-1}$]
E^*	activation energy required to make a diffusional jump [$J\ mol^{-1}$]
f_{app}	apparent initiator efficiency [–]
f_{chem}	intrinsic initiator efficiency [–]
f_k	initiator efficiency in phase k [–]
$f_{H,x}^G$	fractional hole free volume at the glass transition temperature for component x (x = m, p) [–]
G_N^0	shear modulus of the rubbery plateau [$N\ m^{-2}$]
I_k	concentration of initiator molecules in phase k [$mol\ m^{-3}$]
k_{app}	apparent rate coefficient [$mol\ m^{-3}\ s^{-1}$]
k_{diff}	diffusion contribution to the apparent rate coefficient [$mol\ m^{-3}\ s^{-1}$]
k_{chem}	intrinsic rate coefficient [$mol\ m^{-3}\ s^{-1}$]
$k_{d,k}$	initiator decomposition rate coefficient in phase k [s^{-1}]
$k_{tr,k}$	apparent chain transfer to monomer rate coefficient in phase k [$m^3\ mol^{-1}\ s^{-1}$]
$k_{inI,k}$	apparent chain initiation rate coefficient for the primary radicals $R_{0,k}$ in phase k [$m^3\ mol^{-1}\ s^{-1}$]
$k_{inCl,k}$	apparent chain initiation rate coefficient for the Cl radicals in phase k [$m^3\ mol^{-1}\ s^{-1}$]
$k_{p,k}$	apparent propagation rate coefficient in phase k [$m^3\ mol^{-1}\ s^{-1}$]
$k_{r,2}$	initiator derived radical recombination rate coefficient [$m^3\ mol^{-1}\ s^{-1}$]
$k_{tc,k}^{i,j}$	apparent rate coefficient for termination by combination between two radicals R_i and R_j with chain length i and j in phase k [$m^3\ mol^{-1}\ s^{-1}$]
$k_{tc,k}^{I,J}$	apparent rate coefficient for termination by combination between two radicals $R_{I',2}$ and $R_{J',2}$, representing macroradical classes Δ_I and Δ_J [$m^3\ mol^{-1}\ s^{-1}$]
$k_{td,k}^{i,j}$	apparent rate coefficient for termination by disproportionation between two radicals R_i and R_j with chain length i and j in phase k [$m^3\ mol^{-1}\ s^{-1}$]
$k_{td,k}^{I,J}$	apparent rate coefficient for termination by disproportionation between two radicals $R_{I',2}$ and $R_{J',2}$, representing macroradical classes Δ_I and Δ_J [$m^3\ mol^{-1}\ s^{-1}$]
$\langle k_{tc,2}\rangle$	overall apparent termination rate coefficient for termination by combination in phase 2 (Eq. (31)) [$m^3\ mol^{-1}\ s^{-1}$]
$\langle k_{td,2}\rangle$	overall apparent termination rate coefficient for termination by disproportionation in phase 2 (Eq. (31)) [$m^3\ mol^{-1}\ s^{-1}$]
$k_{tCl,k}$	apparent termination rate coefficient between a Cl radical and radicals R_i with chain length i in phase k [$m^3\ mol^{-1}\ s^{-1}$]
K_{11}	free volume parameter of the pure monomer = $\hat{V}_m^0(T_{g,m})\alpha_{l,m}$ [$m^3\ kg^{-1}\ K^{-1}$]
K_{21}	free volume parameter of the pure monomer = $f_{H,m}^G/\alpha_{l,m}$ [K]
M_k	concentration of monomer molecules in phase k [$mol\ m^{-3}$]
mm_m	molecular mass of the monomer [$kg\ mol^{-1}$]
M_{cr}	critical molecular mass for entanglement of the polymer chains [$kg\ mol^{-1}$]
M_i	molecular mass of the polymer molecules with chain length i [$kg\ mol^{-1}$]
M_{mj}	molecular mass of the jumping unit of the monomer (= mm_m) [$kg\ mol^{-1}$]
M_{pj}	molecular mass of the jumping unit of the polymer [$kg\ mol^{-1}$]
$\bar{M}_m$	mass averaged molecular mass of polymer molecules [$kg\ mol^{-1}$]
$\bar{M}_{m,k}$	mass averaged molecular mass of polymer molecules in phase k [$kg\ mol^{-1}$]
$\bar{M}_n$	number averaged molecular mass of polymer molecules [$kg\ mol^{-1}$]
$\bar{M}_{n,k}$	number averaged molecular mass of polymer molecules in phase k [$kg\ mol^{-1}$]
$\bar{M}_z$	z averaged molecular mass of polymer molecules [$kg\ mol^{-1}$]
$\bar{M}_{z,k}$	z averaged molecular mass of polymer molecules in phase k [$kg\ mol^{-1}$]

N_A	Avogadro constant [mol^{-1}]
$P_{i,k}$	concentration of dead polymer molecules with chain length i in phase k [$mol\ m^{-3}$]
R	universal gas constant [$J\ mol^{-1}\ K^{-1}$]
$R_{0,k}$	initiator derived radical (or primary radical) concentration [$mol\ m^{-3}$]
$R_{i,k}$	concentration of (macro)radicals with chain length i in phase k [$mol\ m^{-3}$]
$\langle R^2 \rangle$	mean-square end-to-end distance of the polymer chains [m^2]
$R_{I,2}$	sum of all radical concentrations in class Δ_I [$mol\ m^{-3}$]
$R_{I',2}$	average concentration of radicals belonging to class Δ_I [$mol\ m^{-3}$]
T	temperature [K]
$T_{g,x}$	glass transition temperature of component x (x=Cl, i, m) [K]
$T_{g,m-p}$	glass transition temperature of the monomer–polymer mixture [K]
V_k	volume of phase k [m^3]
$\hat{V}_{FH}$	specific hole free volume of the mixture [$m^3\ kg^{-1}$]
$\hat{V}_{FH,x}$	specific hole free volume of the pure component x (x=m, p) [$m^3\ kg^{-1}$]
$\hat{V}_{FH,x}^G$	specific hole free volume of the pure component x (x=m, p) at the glass transition temperature [$m^3\ kg^{-1}$]
$\hat{V}_W$	van der Waals specific volume [$m^3\ kg^{-1}$]
$\hat{V}_x^*$	specific hole free volume required for the component x to jump (x=i, m, p) ($=\hat{V}_x^0(0)$) [$m^3\ kg^{-1}$]
$\hat{V}_x^0$ or $\hat{V}_x^0(T)$	specific volume of the equilibrium liquid component x (x=i, m, p) (at temperature T) [$m^3\ kg^{-1}$]
$\tilde{V}_x^0(0)$	volume of equilibrium liquid per mole of component x molecules at 0 K [$m^3\ mol^{-1}$]
$\tilde{V}^*$	hole free volume required for a jump per mole of jumping units [$m^3\ mol^{-1}$]
$\tilde{V}_{xj}^*$	hole free volume required for a jump per mole of jumping units of component x (x=Cl, i, m, p) [$m^3\ mol^{-1}$]
$\tilde{V}_{c,x}$	molar volume of component x (x=m, w) at its critical temperature [$m^3\ mol^{-1}$]
$\tilde{V}_{FH}$	hole free volume per mole of all individual jumping units in the mixture [$m^3\ mol^{-1}$]

Greek symbols

$\alpha_{c,p}$	close-packed crystalline state volumetric thermal expansion coefficient [K^{-1}]
$\alpha_{l,x}$	volumetric thermal expansion coefficient of component x (x=m, p) above glass transition temperature [K^{-1}]
γ	average overlap factor for the hole free volume of the mixture [–]
γ_x	overlap factor for the hole free volume of the pure component x (x=m, p) [–]
δ_x	solubility parameter of component x (x=m, p) [$J^{1/2}\ cm^{-3/2}$]
Δ_I	class I of grouped macroradical chain length distribution [–]
$\lvert\Delta_I\rvert$	number of macroradical chain lengths in class I [–]
η	liquid or polymer viscosity [$N\ s\ m^{-2}$]
η_{cr} or $\eta_0(M_{cr})$	polymer zero shear melt viscosity at polymer molecular mass M_{cr} [$N\ s\ m^{-2}$]
$\lambda_{s,k}$	s-th moment of the macroradical chain length distribution in phase k
$\mu_{s,k}$	s-th moment of the polymer chain length distribution in phase k
ρ_p	density of the polymer [$kg\ m^{-3}$]
σ_m	reaction distance [m]
ω_x	mass fraction of component x (x=m, p) in the polymer-rich phase ($k=2$) [–]

Subscripts

app	apparent
diff	diffusion
chem	intrinsic
i	chain length, initiator derived
m	monomer
p	polymer
k	phase, monomer-rich phase ($k=1$), polymer-rich phase ($k=2$)

Superscripts

i, j	chain length
G	property at glass transition temperature
$*$	free volume theory property for diffusional jump

described independently, based on the physical properties of the polymerization mixture [16]. The latter methodology is applied in this paper to estimate the intrinsic rate coefficients for propagation, $k_{p,chem}$, chain transfer to monomer, $k_{tr,chem}$, chain initiation by a Cl radical, $k_{inCl,chem}$, termination between macroradicals, $k_{tc,chem}$ and $k_{td,chem}$, and termination between macroradicals and a Cl radical, $k_{tCl,chem}$, from the experimental data for monomer conversion and moments of the MMD ($\bar{M}_n$, $\bar{M}_m$, $\bar{M}_z$). Although it must be expected that there will always be some influence of the applied diffusion model on the estimated intrinsic rate coefficients, the accuracy of the obtained values for the intrinsic rate parameters increases when the diffusion effects are accounted for independently.

2. Suspension polymerization

The suspension polymerization of vinyl chloride is performed in a batch reactor with the monomer dispersed in water. The dispersion is maintained by adding suspension stabilizers and by stirring. An initiator is dissolved in the monomer phase. Polymerization is started by bringing the reactor to the desired temperature. The reactor is operated at a pressure of about 10 bar, corresponding to the monomer and water vapor pressure.

Three stages are distinguished during the vinyl chloride suspension polymerization process [1–5,17]. Each stage is characterized by the number of phases present in the polymerization reactor. During the first stage the polymerization occurs in the monomer phase, called the monomer-rich phase. Because the polymer is almost insoluble in its monomer, it almost immediately forms a separate phase in the monomer phase, called the polymer-rich phase. This second stage starts at a monomer conversion of about 0.1%. During the second stage, polymerization proceeds both in the monomer-rich phase and the polymer-rich phase. The polymer molecules that are formed in the monomer-rich phase, are transferred to the polymer-rich phase, leading to a constant composition in this phase of approximately 30 wt% of monomer. This composition is determined by the solubility of the monomer in the polymer-rich phase. Due to the constant composition of the polymer-rich phase and the increasing conversion of vinyl chloride, the monomer-rich phase decreases in volume while the polymer-rich phase volume increases. At a conversion of about 65%, named the critical conversion, the monomer-rich phase disappears and the third stage starts. During this stage, polymerization takes place in the polymer-rich phase only, the composition of which now changes due to the further conversion of monomer. As a result the viscosity of this phase increases notably. According to Gibb's phase law, there is a reactor pressure drop during the third stage.

3. Experimental

In this work, batch suspension polymerization experiments are performed in the temperature range of 308–338 K with concentrations of the initiator *tert*-butyl peroxyneodecanoate (TBPD) varying between 0.026 and 3.0 wt%, based on the monomer. Experiments are performed in an agitated 0.002 m^3 stainless steel reactor with 0.7 kg of distilled, deionized water and 0.3 kg of vinyl chloride. After adding the initiator at 298 K, the reactor is heated to the polymerization temperature in about 20 min, while cooling of the reactor to stop the polymerization process takes 2–3 min. The reported polymerization times are defined with respect to the start of the heating of the reactor. The temperature is monitored continuously and accounted for in the calculations.

The monomer conversion is measured gravimetrically. The molecular mass distribution is determined according to the triple detection GPC/SEC principle (Viscotek). The GPC system used in this work includes a HP-1050 pump operating at 1.0 ml/min. A Spectra Physics SP8875 autosampler (Thermo-Finnigan) is used. All injection volumes are 100 μl. All samples are dissolved in THF. The set of columns used to perform the separation consists of a PSS SDV pre-column (length 50 mm, internal diameter 8 mm), a PSS 1000 Å SDV column (length 300 mm, internal diameter 8 mm) and a PSS 10^5 Å SDV column (length 300 mm, internal diameter 8 mm). The temperature during operation is kept constant at 40 °C.

The elution curves are evaluated with Viscotek triple detection, that combines refractive-index, viscosity, and light scattering measurements. A Viscotek model 250 dual detector, consisting of a refractometer and viscometer is employed. The refractometer is operated at 35 °C and at a wavelength of 670 nm. The viscometer is thermostated at 35 °C. A Viscotek model 600 Right Angle Laser Light Scattering detector with a cell volume of 12 μl, operating at 670 nm is used. The results of these measurements are processed using Viscotek Tri-SEC software.

4. Regression analysis

Parameter estimates are obtained by minimizing the objective function S (**b**) with respect to the parameter estimates **b** (b_j, $j=1,\ldots,p$) [18]:

$$S(\mathbf{b}) = \sum_{i=1}^{n} (\mathbf{y}_i - \hat{\mathbf{y}}_i)^T \mathbf{\Sigma}^{-1} (\mathbf{y}_i - \hat{\mathbf{y}}_i) \rightarrow \text{minimum} \tag{1}$$

in which $\mathbf{y}_i$ and $\hat{\mathbf{y}}_i$ ($i=1,\ldots,n$) are the vectors of the observed and the calculated response values of the i-th experiment. Each experiment i includes v responses y_{ik} and $\hat{y}_{ik}$ ($k=1,\ldots,v$). There are 85 experimental observations used for the regression, each providing four responses: Monomer conversion and three moments of the MMD ($\bar{M}_\text{n}, \bar{M}_\text{m}, \bar{M}_\text{z}$) and corresponding to eight sets of conditions, i.e. of combinations of temperature and initiator concentrations. The objective function is minimized with a multi-response Levenberg–Marquardt algorithm [19]. The initial values for the pre-exponential factors and activation energies in the non-isothermal regression are obtained from isothermal parameter estimation. The matrix $\mathbf{\Sigma}^{-1}$ is the inverse of the ($v \times v$) error covariance matrix $\mathbf{\Sigma}$ and contains the weights of the regression. The elements σ_{kl}^2 of $\mathbf{\Sigma}$ are estimated from:

$$\sigma_{kl}^2 = \frac{\sum_{i=1}^{n} (y_{ik} - \hat{y}_{ik})(y_{il} - \hat{y}_{il})}{(nv - p)/v} \tag{2}$$

To start, a diagonal error covariance matrix $\mathbf{\Sigma}$ is applied, calculated from the reciprocal of the squared average magnitude of the responses. It is known that correlation between the experimental errors on the responses can have a significant effect on the parameter estimates. Hence, the parameter estimates obtained by minimization of Eq. (1) with a diagonal error matrix were used to obtain an estimate of the full error covariance matrix using Eq. (2). With the latter the objective function was again minimized leading to a new set of parameter estimates. In the present work, this approach leads to only marginal changes in the values of the parameter estimates.

The model adequacy is tested with duplicate experiments. The statistical significance of the global regression is expressed by the F test, based on the sum of squares of the calculated response values and the residual sum of squares. A high F value corresponds to a high significance of the global regression. The parameter estimates are tested for statistical significance on the basis of their individual t values. The Arrhenius equations for the intrinsic rate coefficients are reparameterized in order to avoid strong binary correlation between the pre-exponential factors and the corresponding activation energies ($\bar{T} = 323$ K):

$$k = A^{*} \exp\left(-\frac{E}{R}\left(\frac{1}{T} - \frac{1}{\bar{T}}\right)\right) \tag{3}$$

5. Kinetic model

In this section, the reactions that are taken into account in the modeling of the suspension polymerization are discussed first. Next, the applied strategy to describe the effect of diffusion on the reaction kinetics is discussed. The mass balances are constructed and the method of moments is used to reduce the large number of mass balances and to calculate the moments of the molecular mass distribution.

5.1. Polymerization reactions

The reactions taken into account for the vinyl chloride suspension polymerization are summarized in Table 1. The reaction scheme is valid in both the monomer-rich phase ($k = 1$) and the polymer-rich phase ($k = 2$). All reactions can be regarded as the result of two consecutive steps. The first is the encounter of two reactant species, which entails the reactants diffusing towards each other. The second is the actual reaction step, in which the reactants overcome an activation barrier. If the rate-determining step is the former, the reaction is diffusion-controlled. If the rate-determining step is the latter, the reaction is reaction-controlled.

Reactions in the polymer-rich phase ($k = 2$) can become diffusion-controlled, while reactions in the monomer-rich phase ($k = 1$) are reaction-controlled. As a result, the observed rate coefficients (also called apparent rate coefficients) in the monomer-rich phase are related to the reaction step only and are equal to the intrinsic rate coefficients. The observed rate coefficient in the polymer-rich phase can be regarded as the sum of a reaction-related term and a diffusion-related term [20], see Eq. (4).

5.2. Combination of reaction and diffusion

The nature of diffusional limitations is similar for all considered reactions. Despite this similarity, the effect of diffusion is often modeled with different expressions for the diffusional effects. In this paper, the effect of diffusion on reaction is modeled following an identical method for all diffusional effects and applied to all the components of the considered reactions. All the apparent rate coefficients, k_{app}, are consistently calculated based on an intrinsic rate coefficient k_{chem} and on a diffusion contribution k_{diff} [20,21]:

Table 1
Vinyl chloride polymerization reactions in the monomer-rich ($k = 1$) and the polymer-rich phase ($k = 2$), with $i, j = 1,\ldots,\infty$

Type of reaction	
Decomposition of the initiator	$I_k \xrightarrow{f_k k_{\mathrm{d},k}} 2R_{0,k}$
Chain initiation	$R_{0,k} + M_k \xrightarrow{k_{\mathrm{inI},k}} R_{1,k}$
Propagation	$R_{i,k} + M_k \xrightarrow{k_{\mathrm{p},k}} R_{i+1,k}$
Chain transfer to monomer	$R_{i,k} + M_k \xrightarrow{k_{\mathrm{tr},k}} P_{i+1,k} + \mathrm{Cl}_k$
Chain initiation by a Cl radical	$\mathrm{Cl}_k + M_k \xrightarrow{k_{\mathrm{inCl},k}} R_{1,k}$
Termination by combination	$R_{i,k} + R_{j,k} \xrightarrow{k_{\mathrm{tc},k}^{i,j}} P_{i+j,k}$
Termination by disproportionation	$R_{i,k} + R_{j,k} \xrightarrow{k_{\mathrm{td},k}^{i,j}} P_{i,k} + P_{j,k}$
Termination with Cl radical	$R_{i,k} + \mathrm{Cl}_k \xrightarrow{k_{\mathrm{tCl},k}} P_{i,k}$

$$\frac{1}{k_{\mathrm{app}}} = \frac{1}{k_{\mathrm{chem}}} + \frac{1}{k_{\mathrm{diff}}} \tag{4}$$

The diffusional contribution k_{diff} is consistently modeled with the Smoluchowski expression for all diffusion-controlled reactions [22]. The diffusion coefficients in this Smoluchowski expression for k_{diff} are calculated based on the physical properties of the components of the mixture with the free volume theory. This approach avoids the need for adjustable diffusion-related parameters. The validity of this strategy to model diffusional limitations in the suspension polymerization of vinyl chloride has been verified by De Roo et al. [16]. Also, in the present approach diffusion limitations are taken into account for all the reactions shown in Table 1, i.e. not limited to initiation, propagation and termination reactions.

The initiator efficiency in the polymer-rich phase is derived by applying the pseudo-steady-state approximation to the initiator derived radicals in their cage $(R_0\cdots \mathrm{CO}_2\cdots R_0)_2$. This results in:

$$\frac{1}{V_2}\frac{\mathrm{d}(V_2 R_{0,2})}{\mathrm{d}t} = 2k_{\mathrm{diff}}(R_0\ldots R_0)_2 = 2k_{\mathrm{diff}}\frac{k_{\mathrm{d},2} I_2}{k_{\mathrm{diff}} + k_{\mathrm{r},2}} \tag{5}$$

and, as by definition,

$$\frac{1}{V_2}\frac{\mathrm{d}(V_2 R_{0,2})}{\mathrm{d}t} = 2 f_2 k_{\mathrm{d},2} I_2 \tag{6}$$

it follows that

$$\frac{1}{f_2} = 1 + \frac{k_{\mathrm{r},2}}{k_{\mathrm{diff}}} \tag{7}$$

The value of $k_{\mathrm{r},2}$ in Eq. (7) is taken equal to 1 $\mathrm{m}^3\ \mathrm{mol}^{-1}\ \mathrm{s}^{-1}$

[45]. The latter value is found for peroxide radicals. A more general expression, analogous to Eq. (4), for the apparent initiator efficiency f_{app} (where $f_{\mathrm{app}}=f_2$) is obtained by introducing the so-called chemical or intrinsic initiator efficiency f_{chem}:

$$\frac{1}{f_{\mathrm{app}}}=\frac{1}{f_{\mathrm{chem}}}+\frac{1(\mathrm{m}^3\ \mathrm{mol}^{-1}\ \mathrm{s}^{-1})}{k_{\mathrm{diff}}} \tag{8}$$

The chemical efficiency, f_{chem}, is defined as the initiator efficiency when no diffusional limitations are present. Its value is determined by the decomposition mechanism of the initiator. The above approach for deriving Eq. (8) implies that $f_{\mathrm{chem}}=1$ (Eq. (7) with $k_{\mathrm{r},2}=1\ \mathrm{m}^3\ \mathrm{mol}^{-1}\ \mathrm{s}^{-1}$). However, for a number of initiators a value smaller than one is proposed semi-empirically: $0\leq f_{\mathrm{chem}}\leq 1$. The initiator (*tert*-butyl peroxyneodecanoate), TBPD, undergoes decarboxylation due to a concerted two-bond scission [23]. Recombination ($k_{\mathrm{r},2}$) produces an inert molecule I_2', resulting in an initiator efficiency smaller than one:

$$\begin{tikzcd} I_2 \arrow[r, "k_{d,2}"] & (R_0\ldots\mathrm{CO}_2\ldots R_0)_2 \arrow[r, "k_{\mathrm{diff}}"] \arrow[d, "k_{r,2}"] & R_{0,2}+R_{0,2} \\ & I_2' & \end{tikzcd} \tag{9}$$

f_{chem} is fixed at 0.7 for all calculations. The diffusion contribution k_{diff} and, therefore, f_2 depends on the initiator, the temperature and the composition of the polymer-rich phase. The initiator efficiency in the monomer-rich phase, f_1, is equal to f_{chem} as no diffusion limitations are considered in the monomer-rich phase. The initiator decomposition rate coefficient $k_{\mathrm{d},k}$ is taken to be equal in both phases and Arrhenius parameter values provided by the initiator manufacturer are used. The initiator partition coefficient between the two phases $K_I=I_2/I_1$ is fixed at 0.77 [1]. Furthermore, the phase equilibria calculations for, e.g. the determination of the composition of the polymer-rich phase, are calculated as described in Kiparissides et al. [3] using the physical properties as given in De Roo et al. [16].

5.2.1. The diffusion contribution

The diffusion contribution for a general reaction of reactants y and z is calculated using the Smoluchowski expression [22]:

$$k_{\mathrm{diff}}=4\pi(r_{\mathrm{y}}+r_{\mathrm{z}})(D_{\mathrm{y}}+D_{\mathrm{z}})N_{\mathrm{A}} \tag{10}$$

$r_{\mathrm{y}}+r_{\mathrm{z}}$ is the distance between the two species when reaction occurs and is taken equal to the Lennard–Jones diameter of a monomer molecule ($\sigma_{\mathrm{m}}=4.69\times10^{-10}\ \mathrm{m}$) for all reactions. ($D_{\mathrm{y}}+D_{\mathrm{z}}$) is the mutual diffusion coefficient consisting of two individual diffusion coefficients of the reacting species y and z [24,25]. The individual diffusion coefficients of the reacting species D_{x} (x = y or z) are the diffusion coefficients of the reactants. For the monomer, the initiator derived radicals and the Cl radicals the D_{x} are the center-of-mass diffusion coefficients D_{x} (cent). For the macroradicals the individual diffusion coefficient D_{x} in Eq. (10) consists of two terms: The center-of-mass diffusion coefficient D_{p}^{i}(cent), depending on the chain length i, and the reaction diffusion coefficient D_{p} (rd), accounting for the movement of the radical chain end during a propagation step. D_{p} (rd) is calculated from:

$$D_{\mathrm{p}}(\mathrm{rd})=\frac{1}{6}k_{\mathrm{p},2}M_2a^2 \tag{11}$$

a is the root-mean-square end-to-end distance per square root of the number of monomer units in a polymer chain ($=6.09\times10^{-10}\ \mathrm{m}$). The centre-of-mass diffusion coefficients D_{x} (cent) are calculated as the self-diffusion coefficients, using the free volume theory. For the monomer, the initiator derived radicals and the Cl radicals the self-diffusion coefficients are written as D_{m}, D_{i} and D_{Cl}. For the macroradical the individual diffusion coefficient in Eq. (10) is written as $D_{\mathrm{p+rd}}^{i}$.

$$D_{\mathrm{p+rd}}^{i}=D_{\mathrm{p}}^{i}+D_{\mathrm{p}}(\mathrm{rd}) \tag{12}$$

where D_{p}^{i} is the self-diffusion coefficient of a macroradical $R_{i,2}$ with chain length i. Applying the above, the diffusion contributions k_{diff} to the apparent rate coefficients for initiator decomposition, propagation, chain transfer to monomer, chain initiation by a Cl radical and termination are obtained from the following expressions:

$$\text{decomposition}\quad k_{\mathrm{diff}}=4\pi\sigma_{\mathrm{m}}(2D_{\mathrm{i}})N_{\mathrm{A}} \tag{13}$$

$$\text{propagation, chain transfer}\quad k_{\mathrm{diff}}=4\pi\sigma_{\mathrm{m}}D_{\mathrm{m}}N_{\mathrm{A}} \tag{14}$$

$$\text{initiation by a Cl radical}\quad k_{\mathrm{diff}}=4\pi\sigma_{\mathrm{m}}(D_{\mathrm{m}}+D_{\mathrm{Cl}})N_{A} \tag{15}$$

combination, disproportionation

$$k_{\mathrm{diff}}^{i,j}=2\pi\sigma_{\mathrm{m}}\left(D_{\mathrm{p+rd}}^{i}+D_{\mathrm{p+rd}}^{j}\right)N_{\mathrm{A}} \tag{16}$$

$$\text{Cl termination}\quad k_{\mathrm{diff}}=2\pi\sigma_{\mathrm{m}}D_{\mathrm{Cl}}N_{\mathrm{A}} \tag{17}$$

5.2.2. Calculation of self-diffusion coefficients

The self-diffusion coefficients for the monomer (D_{m}), the macroradicals with chain length i (D_{p}^{i}), the initiator primary radicals (D_{i}) and the Cl radicals (D_{Cl}) are calculated with the free volume theory [26–28]:

$$D_{\mathrm{x}}=D_{\mathrm{x},0}\exp\left(-\frac{E^*}{RT}\right)\exp\left(-\frac{\tilde{V}_{\mathrm{xj}}^{*}}{\tilde{V}_{\mathrm{FH}}/\gamma}\right) \qquad \mathrm{x}=\mathrm{Cl},\mathrm{i},\mathrm{m} \tag{18}$$

$$D_{\mathrm{p}}^{i}=\bar{D}_{\mathrm{p},0}\exp\left(-\frac{\tilde{V}_{\mathrm{pj}}^{*}}{\tilde{V}_{\mathrm{FH}}/\gamma}\right) \tag{19}$$

The self-diffusion coefficients are determined by three parameters: (1) A pre-exponential factor, (2) an activation energy E^* representing the energy required to make a diffusional jump and (3) a free volume contribution representing the availability of free volume for diffusion. The macroradical diffusion coefficient pre-exponential factor accounts for the molecular mass dependency. $\tilde{V}^*_{\mathrm{xj}}$ ($\mathrm{x}=\mathrm{Cl, i, m, p}$) is the molar volume a molecule needs to make a diffusional jump. $\tilde{V}_{\mathrm{FH}}$ is the hole free volume of the polymer–monomer mixture of the polymer-rich phase available for diffusion and γ is the overlap factor ($0.5 \le \gamma \le 1$, [29]). This factor is needed to take into account the overlap between volume elements. The free volume contributions in Eqs. (18) and (19) allow to account for the concentration and most of the temperature dependency. This results from the dependency of $\tilde{V}_{\mathrm{FH}}/\gamma$ on the mass fraction of the polymer in the polymer-rich phase ω_{p} and on the temperature. The temperature dependency follows from the thermal expansion properties of the monomer and the polymer in the monomer–polymer mixture. The ratio of $\tilde{V}_{\mathrm{FH}}/\gamma$ can be calculated from:

$$\frac{\tilde{V}_{\mathrm{FH}}}{\gamma} = \frac{\tilde{V}_{\mathrm{FH}}/\gamma}{(\omega_{\mathrm{m}}/M_{\mathrm{mj}}) + (\omega_{\mathrm{p}}/M_{\mathrm{pj}})} \tag{20}$$

M_{mj} and M_{pj} are the molecular mass of the monomer and macroradical jumping unit and ω_{m} and ω_{p} are the monomer and polymer mass fraction in the polymer-rich phase. $\tilde{V}^*_{\mathrm{xj}}$ can also be expressed as $\hat{V}^*_{\mathrm{x}} M_{\mathrm{xj}}$, with $\hat{V}^*_{\mathrm{x}}$ the specific volume that a molecule needs to make a diffusional jump. $\hat{V}_{\mathrm{FH}}$ is the specific hole free volume and is calculated from the physical properties of the mixture ($T_{\mathrm{g,m-p}} \le T \le T_{\mathrm{g,p}}$) [28]

$$\frac{\hat{V}_{\mathrm{FH}}}{\gamma} = \omega_{\mathrm{m}} \frac{\hat{V}^0_{\mathrm{m}}(T_{\mathrm{g,m}})}{\gamma_{\mathrm{m}}} \left(f^{\mathrm{G}}_{\mathrm{H,m}} + \int_{T_{\mathrm{g,m}}}^{T} \alpha_{\mathrm{l,m}} \mathrm{d}T' \right) + \omega_{\mathrm{p}} \frac{\hat{V}^0_{\mathrm{p}}(T_{\mathrm{g,p}})}{\gamma_{\mathrm{p}}} \left(f^{\mathrm{G}}_{\mathrm{H,p}} - (\alpha_{\mathrm{l,p}} - \alpha_{\mathrm{c,p}})(T_{\mathrm{g,p}} - T) \right) \tag{21}$$

The temperature dependency of the monomer thermal expansion coefficient $\alpha_{\mathrm{l,m}}$ is taken into account while for the polymer the liquid thermal expansion coefficient $\alpha_{\mathrm{l,p}}$ can be considered constant over the considered temperature range. $T_{\mathrm{g,x}}$ ($\mathrm{x}=\mathrm{m, p}$) and $T_{\mathrm{g,m-p}}$ are the glass transition temperatures of the pure monomer, the pure polymer and the monomer–polymer mixtures. For $T_{\mathrm{g,p}} \le T$, $(\alpha_{\mathrm{l,p}} - \alpha_{\mathrm{c,p}})$ is replaced with $\alpha_{\mathrm{l,p}}$ [28]. $f^{\mathrm{G}}_{\mathrm{H,x}}$ and $\hat{V}^0_{\mathrm{x}}(T_{\mathrm{g,x}})$ are the fractional hole free volume and the specific volume of the pure component ($\mathrm{x}=\mathrm{m, p}$) at $T_{\mathrm{g,x}}$. γ_{x} is the hole free volume overlap factor. The close-packed crystalline state expansion coefficient $\alpha_{\mathrm{c,p}}$ is calculated from Eq. (22) [28].

$$\alpha_{\mathrm{c,p}} = \frac{1}{T_{\mathrm{g,p}}} \ln \left(\frac{\hat{V}^0_{\mathrm{p}}(T_{\mathrm{g,p}})(1 - f^{\mathrm{G}}_{\mathrm{H,p}})}{\hat{V}^0_{\mathrm{p}}(0)} \right) \tag{22}$$

5.2.3. Calculation of diffusion related parameters

5.2.3.1. Pre-exponential factors. $D_{\mathrm{m,0}}$ is calculated with the Dullien equation [27,28,30]:

$$D_{\mathrm{m,0}} = \frac{0.124 \times 10^{-16} \tilde{V}^{2/3}_{\mathrm{c,m}} RT}{\mathrm{mm}_{\mathrm{m}} \eta \hat{V}^0_{\mathrm{m}}} \exp\left(\frac{\gamma_{\mathrm{m}} \hat{V}^*_{\mathrm{m}}/K_{11}}{K_{21} - T_{\mathrm{g,m}} + T} \right) = 1.14 \times 10^{-7} m^2 s^{-1} \tag{23}$$

in which $K_{11}/\gamma_{\mathrm{m}}$ and K_{21} are the monomer free volume parameters, equal to $\hat{V}^0_{\mathrm{m}}(T_{\mathrm{g,m}})\alpha_{\mathrm{l,m}}/\gamma_{\mathrm{m}}$ and $f^{\mathrm{G}}_{\mathrm{H,m}}/\alpha_{\mathrm{l,m}}$, respectively and calculated as such (Table 2). $\tilde{V}_{\mathrm{c,m}}$ ($=179 \times 10^{-6}$ $\mathrm{m^3\ mol^{-1}}$, [31]) and mm_{m} are the monomer molar critical volume and molecular mass; η and $\hat{V}^0_{\mathrm{m}}$ are the pure monomer viscosity and volume. Despite the presence of

Table 2
Physical properties and free volume properties of the monomer and the polymer

Property	Units	x = m (monomer)	x = p (polymer)
$\rho_{\mathrm{x}} = 1/\hat{V}^{0}_{\mathrm{x}}$ [a,b]	$[\mathrm{kg\ m^{-3}}]$	$94.469/0.2707^{1+(1-T(\mathrm{K})/432)^{0.2716}}$	$1394 - 0.203(T - 273.15) - 2.19 \times 10^{-3} (T - 273.15)^2$
η [c]	$[\mathrm{N\ m^{-2}\ s}]$	$10^{-3}\exp(9.373 - 648.32/T - 4.294 \times 10^{-2} T + 4.316 \times 10^{-5} T^2)$	–
$\hat{V}^*_{\mathrm{x}} = \hat{V}^0_{\mathrm{x}}(0)$ [d]	$[\mathrm{m^3\ kg^{-1}}]$	7.94×10^{-4}	6.66×10^{-4}
$\tilde{V}^*_{\mathrm{xj}} = \tilde{V}^0_{\mathrm{x}}(0)$ [d,e]	$[\mathrm{m^3\ mol^{-1}}]$	49.6×10^{-6}	132.85×10^{-6}
$f^{\mathrm{G}}_{\mathrm{H,x}}$ [f]	[–]	0.025	0.025
$\alpha_{\mathrm{l,x}}$ [a,g]	$[\mathrm{K^{-1}}]$	1.42×10^{-3}	5.85×10^{-4}
$T_{\mathrm{g,x}}$	[K]	70	353.15
γ_{x}	[–]	1.0	1.0
E^*	$[\mathrm{J\ mol^{-1}}]$	16,400	0.0
δ_{x} [d]	$[(\mathrm{J\ m^{-3}})^{1/2}]$	16.19×10^3	19.73×10^3
mm_{m}	$[\mathrm{kg\ mol^{-1}}]$	0.0625	–

[a] Ref. [32].
[b] Ref. [33].
[c] Fitted equation with 213–413 K data from Ref. [34].
[d] Ref. [35].
[e] Eq. (28).
[f] Ref. [36].
[g] Ref. [37].

temperature in Eq. (23), the value of $D_{m,0}$ does not strongly depend on temperature and can be considered constant. The pre-exponential factors $D_{c,0}$ and $D_{i,0}$ are taken equal to $D_{m,0}$. This assumption is made since no better means are available. The pre-exponential factor of the polymer diffusion coefficient $\bar{D}_{p,0}$ is determined by calculating the polymer diffusion coefficient at $\omega_p = 1$ and setting this coefficient equal to the diffusion coefficient derived from the reptation theory [38]. Because the polymer-rich phase is a concentrated solution over the entire conversion range, it is expected that $D_p^i \propto M_i^{-2}$. As the free volume theory can be best applied in concentrated or highly concentrated solutions [39], it should equal the melt diffusion coefficient as described by the reptation theory. The reptation diffusion coefficient $D^i_{\text{reptation}}$ is calculated from Refs. [40,41]:

$$D^i_{\text{reptation}} = \frac{G_N^0}{135}\left(\frac{\rho_p RT}{G_N^0}\right)^2\left(\frac{\langle R^2\rangle}{M_i}\right)\frac{M_{cr}}{M_i^2\eta_{cr}} \tag{24}$$

in which G_N^0 is the shear modulus of the rubbery plateau. $\langle R^2\rangle$ is the mean square end-to-end distance of the polymer chain with molecular mass $M_i = \text{mm}_m i$ and density ρ_p. η_{cr} (or η_0 (M_{cr})) is the zero shear melt viscosity at the critical molecular mass of the polymer M_{cr}. In Table 3, the values and expression for the physical properties used in the calculation of $D^i_{\text{reptation}}$ in Eq. (24) are given. The two expressions are set equal at $1.2T_{g,p}$ and solved for $\bar{D}_{p,0}$. At this temperature both theories are valid and the physical properties required for the diffusion coefficients calculations are known. At $T = T_{g,p}$ a lot of physical properties change drastically implying a higher degree of incertainty.

$$D^i_{\text{reptation}}|_{\omega_p=1;\ T=1.2T_{g,p}} = D^i_p|_{\omega_p=1; T=1.2T_{g,p}} \tag{25}$$

From Eq. (25) one obtains:

$$\bar{D}_{p,0} = \frac{6.53\times10^{-10}}{M_i^{1.892}} = \frac{1.24\times10^{-7}}{i^{1.892}} \tag{26}$$

5.2.3.2. Activation energy. E^* is estimated from an experimentally determined plot of E^* as a function of the solubility parameters δ_m and δ_p and the molar volume of the pure solvent $\tilde{V}_m^0$ [m^3 mol^{-1}] at a reference temperature (293 K) [28]. A fit of this plot (Eq. (27), [43]) is used to calculate E^*. E^* equals 16.4 kJ mol^{-1} (Table 2) and is used in the calculation of all D_x.

$$\log E^* = 0.8988\ \ln\left(\log\left(\frac{(\delta_m-\delta_p)^2\tilde{V}_m^0}{4.1868}\right)\right) + 3.4575 \tag{27}$$

Table 3
Values and expressions for physical properties used in the reptation theory diffusion coefficient $D^i_{\text{reptation}}$ (Eq. (24))

Parameter	Units	Value/expression
$G_N^{0\ a}$	[N m^{-2}]	1.5×10^6
M_{cr} [b,c]	[kg mol^{-1}]	6.25
$\langle R^2\rangle^{1/2}$ (this study)	[m]	$2.83\times10^{-9}M_i^{0.554}$
$\log \eta_{cr}(1.2T_{g,p})$ [b]	[N m^{-2} s]	3.89

[a] $G_N^0(T) = 2\rho(T)RT/M_{cr}$.
[b] Ref. [35].
[c] Ref. [42].

5.2.3.3. Free volume parameters. Calculated diffusion coefficients, based on the free volume theory, require the knowledge of detailed volumetric and physical properties of the monomer and the polymer. Their temperature relationships are obtained from correlations (Table 2), while the jump volumes $\tilde{V}^*_{xj}$($x = \text{Cl, i, m, p}$) are calculated as the size of the jump units at 0 K obtained from group contribution methods [26–28]. The monomer jump volume $\tilde{V}^*_{mj}$ is the volume of the molecule itself while the polymer jump segment can be calculated from Eq. (28) [28,43].

$$\tilde{V}^*_{pj} = 0.6224\times10^{-6}T_{g,p} - 86.95\times10^{-6} \tag{28}$$

The primary radical jump unit is calculated as the volume of the largest primary radical at 0 K($=158.1\times10^{-6}$ m^3 mol^{-1}). The Cl radicals have a jump unit volume equal to 19.3×10^{-6} m^3 mol^{-1}. The fractional hole free volume at the glass transition temperature $f^G_{H,x}$($x = \text{m, p}$) is derived from the Williams–Landel–Ferry (WLF) equation. Other important free volume parameters are the overlap factors γ_m and γ_p. For γ_m it is suggested to regress viscosity–temperature (η) and density–temperature $\hat{V}_m^0$ data of the pure monomer with Eq. (23) to obtain the values for the parameters K_{11}/γ_m, $K_{21} - T_{g,m}$ and $D_{m,0}$. However, no statistically significant results could be obtained from this regression due to the strong correlation between these parameters, even after reparameterization of the exponentional term. Furthermore, as several good fits of the experimental data could be obtained with sets of different parameter values, these regression results are not used as such. The main conclusion that could be drawn from the regression was that γ_m is close to one or should be even higher. Theoretically the maximum value of γ_m is 1, hence γ_m is taken equal to one. γ_p can be calculated from Eq. (29) [28].

$$\gamma_p = \frac{\hat{V}_p(T_{g,p})}{K_{12}/\gamma_p} \tag{29}$$

with

$$\frac{K_{12}}{\gamma_p} = \frac{\hat{V}_p^*}{2.303C_1C_2} \tag{30}$$

$C_1 = 19.84$ and $C_2 = 43.89$ are the WLF constants for the polymer [33]. The resulting value for γ_p is also higher than one. Therefore, the maximum value of one is used in all calculations.

5.3. Model equations

The mass balances for the different components involved

Table 4

Mass balances for the different components in the suspension polymerization of vinyl chloride in the monomer-rich ($k=1$) and the polymer-rich phase ($k=2$). Stage 1: $k=1$; stage 2: $k=1, 2$; stage 3: $k=2$. $I_1=I_{t=0}$, $M_1=M_{t=0}$ at $t=0$; $R_{i,1}$, $P_{i,1}=0$ at $t=0$; $R_{i,2}$, $P_{i,2}=0$ at start of stage 2 (monomer conversion$=$0.1%)

Initiator

$$\frac{1}{V_k}\frac{\mathrm{d}(V_kM_k)}{\mathrm{d}t}=-k_{\mathrm{d},k}I_k$$

Monomer

$$\frac{1}{V_k}\frac{\mathrm{d}(V_kM_k)}{\mathrm{d}t}=-2f_kk_{\mathrm{d},k}I_k-(k_{\mathrm{p},k}+k_{\mathrm{tr},k})\sum_{i=1}^{\infty}R_{i,k}M_k-K_{\mathrm{inCl},k}\mathrm{Cl}_kM_k$$

Macroradicals $R_{i,k}(i=1,\ldots,\infty)$

$$\frac{1}{V_k}\frac{\mathrm{d}(V_kR_{1,k})}{\mathrm{d}t}=-2f_kk_{\mathrm{d},k}I_k-k_{\mathrm{p},k}R_{1,k}M_k-k_{\mathrm{tr},k}R_{1,k}M_k+k_{\mathrm{inCl},k}\mathrm{Cl}_kM_k-2R_{1,k}\sum_{j=1}^{\infty}\left(k_{\mathrm{tc},k}^{1,j}+k_{\mathrm{td},k}^{1,j}\right)R_{j,k}-2k_{\mathrm{tCl},k}R_{1,k}\mathrm{Cl}_k$$

$$\frac{1}{V_k}\frac{\mathrm{d}(V_kR_{i,k})}{\mathrm{d}t}=k_{\mathrm{p},k}M_k(R_{i-1,k}-R_{i,k})-k_{\mathrm{tr},k}R_{i,k}M_k-2R_{i,k}\sum_{j=1}^{\infty}\left(k_{\mathrm{tc},k}^{i,j}+k_{\mathrm{td},k}^{i,j}\right)R_{j,k}-2k_{\mathrm{tCl},k}R_{i,k}\mathrm{Cl}_k$$

Polymer molecules $P_{i,k}(i=1,\ldots,\infty)$

$$\frac{1}{V_k}\frac{\mathrm{d}(V_kP_{1,k})}{\mathrm{d}t}=2k_{\mathrm{tCl},k}R_{1,k}\mathrm{Cl}_k$$

$$\frac{1}{V_k}\frac{\mathrm{d}(V_kP_{i,k})}{\mathrm{d}t}=-2k_{\mathrm{tCl},k}R_{i,k}\mathrm{Cl}_k+k_{\mathrm{tr},k}R_{i-1,k}M_k+\sum_{j=1}^{i=1}k_{\mathrm{tc},k}^{j,i-j}R_{j,k}R_{i-j,k}+R_{i,k}\sum_{j=1}^{\infty}k_{\mathrm{td},k}^{i,j}R_i$$

in the reactions shown in Table 1 are given in Table 4. The pseudo-steady-state approximation is applied to the $R_{0,k}$ radicals. This implies that the rate coefficient corresponding to the chain initiation reaction by an initiator derived radical ($k_{\mathrm{inI},k}$) is no longer present in the balances. The mass balance for the monomer in both phases allows the calculation of the monomer conversion. The method of moments is applied to calculate the average properties ($\bar{M}_\mathrm{n}$, $\bar{M}_\mathrm{m}$, $\bar{M}_\mathrm{z}$) of the molecular mass distribution (Table 5). In these equations, the pseudo-steady-state approximation is applied to both the Cl_k and the $R_{0,k}$ radicals. The corresponding initial conditions are also given in Tables 4 and 5, where $t=0$ corresponds with the start of the heating of the reactor. The polymer moments in each phase ($\bar{M}_{\mathrm{n},k}, \bar{M}_{\mathrm{m},k}, \bar{M}_{\mathrm{z},k}$ with $k=1, 2$) are calculated from the ratio $\mu_{s+1,k}/\mu_{s,k}(s=0, 1, 2)$ and are combined according to Xie et al. [2] to calculate the total moments of the MMD.

Note that no energy equations are given. The calculations of the monomer conversion (Table 4) and the moments of the MMD (Table 5) account for the experimentally measured temperatures..

The apparent rate coefficients for termination by combination and disproportionation, $k_{\mathrm{tc},2}^{i,j}$ and $k_{\mathrm{td},2}^{i,j}$, are considered to be chain length dependent. This follows from the chain length dependent diffusion of a macroradical $R_{\mathrm{i},2}$, that is explicitly taken into account in the calculation of a chain length dependent diffusion coefficient, incorporated in $k_{\mathrm{diff}}^{i,j}$ (Eq. (16)).

The overall termination rate coefficients for combination and disproportionation in the polymer-rich phase, $\langle k_{\mathrm{tc},2}\rangle$ and $\langle k_{\mathrm{td},2}\rangle$, are calculated from:

$$\langle k_{\mathrm{tc},2}\rangle=\frac{\sum_{i=1}^{\infty}\sum_{j=1}^{\infty}k_{\mathrm{tc},2}^{i,j}R_{i,2}R_{j,2}}{\left(\sum_{i=1}^{\infty}R_{i,2}\right)^2}$$

$$\langle k_{\mathrm{td},2}\rangle=\frac{\sum_{i=1}^{\infty}\sum_{j=1}^{\infty}k_{\mathrm{td},2}^{i,j}R_{i,2}R_{j,2}}{\left(\sum_{i=1}^{\infty}R_{i,2}\right)^2} \quad (31)$$

The calculation of these overall termination rate coefficients, as well as the calculation of the termination related terms in the higher order moment equations, requires the knowledge of the concentration of macroradicals $R_{i,2}$. These values are obtained by solving the algebraic equations resulting from the application of the pseudo-steady-state approximation to the macroradicals $R_{i,2}$ [44]. Since the macroradical chain length i in vinyl chloride suspension polymerization covers a range of one to theoretically infinity but in practice approximately 20,000, the number of equations to be solved simultaneously is large. Therefore, a coarse graining technique is applied [24,25]. According to this technique, the macroradical distribution is truncated at a reasonable maximum chain length and divided into a

Table 5

Equations for the moments of the macroradical distribution ($\lambda_{s,k}$, $s=0,\ldots,3$) and the polymer molecule distribution ($\mu_{s,k}$, $s=0,\ldots,3$) in the monomer-rich phase ($k=1$) and in the polymer-rich phase ($k=2$). $\lambda_{s,1}$, $\mu_{s,1}=0$ at $t=0$; $\lambda_{s,2}$, $\mu_{s,2}=0$ at start of stage 2 (monomer conversion$=$0.1%)

$$\frac{1}{V_k}\frac{\mathrm{d}(V_k\lambda_{0,k})}{\mathrm{d}t}=2f_kk_{\mathrm{d},k}I_k-2(\langle k_{\mathrm{tc},k}\rangle+\langle k_{\mathrm{td},k}\rangle)\lambda_{0,k}^2-4k_{\mathrm{tCl},k}\lambda_{0,k}\mathrm{Cl}_k$$

$$\frac{1}{V_k}\frac{\mathrm{d}(V_k\lambda_{1,k})}{\mathrm{d}t}=2f_kk_{\mathrm{d},k}I_k-2\sum_{i=1}^{\infty}iR_{i,k}\sum_{j=1}^{\infty}\left(k_{\mathrm{tc},k}^{i,j}+k_{\mathrm{td},k}^{i,j}\right)R_{j,k}-2k_{\mathrm{tCl},k}(\lambda_{0,k}+\lambda_{1,k})\mathrm{Cl}_k+k_{\mathrm{p},k}M_k\lambda_{0,k}+k_{\mathrm{tr},k}M_k(\lambda_{0,k}-\lambda_{1,k})$$

$$\frac{1}{V_k}\frac{\mathrm{d}(V_k\lambda_{2,k})}{\mathrm{d}t}=2f_kk_{\mathrm{d},k}I_k-2\sum_{i=1}^{\infty}i^2R_{i,k}\sum_{j=1}^{\infty}\left(k_{\mathrm{tc},k}^{i,j}+k_{\mathrm{td},k}^{i,j}\right)R_{j,k}-2k_{\mathrm{tCl},k}(\lambda_{0,k}+\lambda_{1,k})\mathrm{Cl}_k+k_{\mathrm{p},k}M_k(\lambda_{0,k}+2\lambda_{1,k})+k_{\mathrm{tr},k}M_k(\lambda_{0,k}-\lambda_{2,k})$$

$$\frac{1}{V_k}\frac{\mathrm{d}(V_k\lambda_{3,k})}{\mathrm{d}t}=2f_kk_{\mathrm{d},k}I_k-2\sum_{i=1}^{\infty}i^3R_{i,k}\sum_{j=1}^{\infty}\left(k_{\mathrm{tc},k}^{i,j}+k_{\mathrm{td},k}^{i,j}\right)R_{j,k}-2k_{\mathrm{tCl},k}(\lambda_{0,k}+\lambda_{3,k})\mathrm{Cl}_k+k_{\mathrm{p},k}M_k(\lambda_{0,k}+3\lambda_{1,k}+3\lambda_{2,k})+k_{\mathrm{tr},k}M_k(\lambda_{0,k}-\lambda_{3,k})$$

$$\frac{1}{V_k}\frac{\mathrm{d}(V_k\mu_{0,k})}{\mathrm{d}t}=(\langle k_{\mathrm{tc},k}\rangle+\langle k_{\mathrm{td},k}\rangle)\lambda_{0,k}^2+2k_{\mathrm{tCl},k}\lambda_{0,k}\mathrm{Cl}_k+k_{\mathrm{tr},k}M_k\lambda_{0,k}$$

$$\frac{1}{V_k}\frac{\mathrm{d}(V_k\mu_{1,k})}{\mathrm{d}t}=\sum_{i=1}^{\infty}i\sum_{j=1}^{i-1}k_{\mathrm{tc},k}^{j,i-j}R_{j,k}R_{i-j,k}+\sum_{i=1}^{\infty}i\sum_{j=1}^{\infty}k_{\mathrm{td},k}^{i,j}R_{i,k}R_{j,k}+2k_{\mathrm{tCl},k}\lambda_{1,k}\mathrm{Cl}_k+k_{\mathrm{tr},k}M_k(\lambda_{0,k}+\lambda_{1,k})$$

$$\frac{1}{V_k}\frac{\mathrm{d}(V_k\mu_{2,k})}{\mathrm{d}t}=\sum_{i=1}^{\infty}i^2\sum_{j=1}^{i-1}k_{\mathrm{tc},k}^{j,i-j}R_{j,k}R_{i-j,k}+\sum_{i=1}^{\infty}i^2R_{i,k}\sum_{j=1}^{\infty}k_{\mathrm{td},k}^{i,j}R_{j,k}+2k_{\mathrm{tCl},k}\lambda_{2,k}\mathrm{Cl}_k+k_{\mathrm{tr},k}M_k(\lambda_{0,k}+2\lambda_{1,k}+\lambda_{2,k})$$

$$\frac{1}{V_k}\frac{\mathrm{d}(V_k\mu_{3,k})}{\mathrm{d}t}=\sum_{i=1}^{\infty}i^3\sum_{j=1}^{i-1}k_{\mathrm{tc},k}^{j,i-j}R_{j,k}R_{i-j,k}+\sum_{i=1}^{\infty}i^2R_{i,k}\sum_{j=1}^{\infty}k_{\mathrm{td},k}^{i,j}R_{j,k}+2k_{\mathrm{tCl},k}\lambda_{3,k}\mathrm{Cl}_k+k_{\mathrm{tr},k}M_k(\lambda_{0,k}+3\lambda_{1,k}+3\lambda_{2,k}+\lambda_{3,k})$$

number of classes $\varDelta_I$, covering a range of chain lengths $|\varDelta_I|$. The macroradicals in one class are assumed to have identical properties. The width of a class $\varDelta_I$ varies as a function of the chain length i. For small chain lengths, a class contains only one chain length ($|\varDelta_I|=1$), for higher chain lengths the classes become broader ($|\varDelta_I|>1$). This is acceptable, since there is no difference from kinetic viewpoint between a macroradical of chain length 1000 and 1001. The radical concentration of a class $\varDelta_I$, $R_{I,2}$, is defined as:

$$R_{I,2}=\sum_{i\in\varDelta_I}R_{i,2}\approx R_{I',2}|\varDelta_I| \tag{32}$$

in which $R_{I',2}$ is the average radical concentration of all radicals belonging to class $\varDelta_I$ ($R_{i,2}=R_{I',2}$, $i\in\varDelta_I$). This approximation is valid if $R_{i,2}$ varies slowly as a function of chain length $i\in\varDelta_I$. By grouping a number of chain lengths into a class, the mass balances for the macroradicals $R_{i,2}$ are transformed into mass balances for the group of macroradicals in a class $\varDelta_I$, $R_{I,2}$. For the first class $\varDelta_1$ and for the following classes $\varDelta_I$ of the distribution this becomes:

$$\begin{aligned}\frac{1}{V_2}\frac{\mathrm{d}(V_2R_{1,2})}{\mathrm{d}t}&=2f_2k_{\mathrm{d},2}I_2-k_{\mathrm{p},2}R_{1,2}M_2-k_{\mathrm{tr},2}R_{1,2}M_2\\&\quad+k_{\mathrm{p},2}\mathrm{Cl}_2M_2\\&\quad-2R_{1,2}\sum_{J=1}^{\infty}\left(k_{\mathrm{tc},2}^{1,J}+k_{\mathrm{td},2}^{1,J}R_{J,2}-2k_{\mathrm{tCl},2}R_{1,2}\mathrm{Cl}_2\right)\end{aligned} \tag{33}$$

$$\begin{aligned}\frac{1}{V_2}\frac{\mathrm{d}(V_2R_{I,2})}{\mathrm{d}t}&=\frac{k_{\mathrm{p},2}M_2R_{I-1,2}}{|\varDelta_{I-1}|}-\frac{k_{\mathrm{p},2}M_2R_{I,2}}{|\varDelta_I|}\\&\quad-k_{\mathrm{tr},2}R_{I,2}M_2\\&\quad-2R_{I,2}\sum_{J=1}^{\infty}\left(k_{\mathrm{tc},2}^{I,J}+k_{\mathrm{td},2}^{I,J}\right)R_{J,2}\\&\quad-2k_{\mathrm{tCl},2}R_{I,2}\mathrm{Cl}_2\end{aligned} \tag{34}$$

From the application of the pseudo-steady-state approximation to the macroradical classes $R_{I,2}$ the following equations are obtained:

$$R_{1,2}=\frac{2f_2k_{\mathrm{d},2}I_2+k_{\mathrm{p},2}\mathrm{Cl}_2M_2}{k_{\mathrm{p},2}M_2+k_{\mathrm{tr},2}M_2+2\sum_{J=1}^{\infty}\left(k_{\mathrm{tc},2}^{I,J}+k_{\mathrm{td},2}^{I,J}\right)R_{J,2}+2k_{\mathrm{tCl},2}\mathrm{Cl}_2} \tag{35}$$

$$R_{I,2}=\frac{k_{\mathrm{p},2}M_2R_{I-1,2}/|\varDelta_{I-1}|}{(k_{\mathrm{p},2}M_2)/|\varDelta_I|+k_{\mathrm{tr},2}M_2+2\sum_{J=1}^{\infty}\left(k_{\mathrm{tc},2}^{I,J}+k_{\mathrm{td},2}^{I,J}\right)R_{J,2}+2k_{\mathrm{tCl},2}\mathrm{Cl}_2} \tag{36}$$

In these equations, the $R_{I,2}$ remain a function of the macroradical concentrations $R_{I,2}$ in class $\varDelta_I$ because of the summation in the denominator. Therefore, the Eqs. (35) and (36) are solved in an iterative cycle until convergence is reached. Convergence is tested for the calculated overall termination by combination and disproportionation rate coefficients, $\langle k_{\mathrm{tc},2}\rangle$ and $\langle k_{\mathrm{td},2}\rangle$, the total radical concentration, the number averaged and the mass averaged moments of the macroradical distribution. The relative tolerance is set equal to 10^{-6}.

The overall termination rate coefficients can only be used for the calculation of the zeroth order moment equations. For higher order moments, however, the termination related terms can no longer be written as a function of the overall termination coefficients and the total radical concentrations. The summations have to be calculated rigorously in order to correctly take into account the chain length dependent nature of the termination processes.

6. Regression results

6.1. Parameter estimates

The Arrhenius parameters of the intrinsic rate coefficients for propagation, chain transfer to monomer, chain initiation by a Cl radical, termination by combination and disproportionation and termination with Cl radicals were estimated. The activation energies of the intrinsic termination by combination reactions, E_{tc} and E_{tCl}, could not be estimated significantly and were fixed at zero. Termination by combination is the dominant termination mechanism. This conclusion is based on the following argumentation. The termination between two macroradicals with chain length i and j, $R_{i,k}$ and $R_{j,k}$, was assumed to occur by both combination and disproportionation, with apparent rate coefficients $k_{\mathrm{tc},k}^{i,j}$ and $k_{\mathrm{td},k}^{i,j}$. However, no statistically significant estimates for the Arrhenius parameters corresponding to the termination by disproportionation reaction were obtained during the regression of the experimental data. The correlation of parameters corresponding to the termination by disproportionation reaction with parameters corresponding to other reactions was smaller than 0.9 allowing to conclude that termination occurs predominantly by combination. Note that, according to the terminology introduced in Table 1, the chain transfer to monomer reaction is not considered to be a termination reaction. The 10 remaining estimated parameter values and their 95% confidence intervals are given in Table 6. The error covariance matrix and the related error correlation matrix

Table 6
Estimates of the reparameterized pre-exponential factor and activation energy of the intrinsic rate coefficients for propagation, $k_{\mathrm{p,chem}}$, for chain transfer to monomer, $k_{\mathrm{tr,chem}}$, for termination, $k_{\mathrm{tc,chem}}$ and $k_{\mathrm{tCl,chem}}$, and for chain initiation by a Cl radical, $k_{\mathrm{inCl,chem}}$ with their 95% confidence limits (rate coefficient $k = A^* \exp((-E/R)((1/T) - (1/\bar{T})))$ and $\bar{T} = 323$ K)

Rate coefficient	A^* [m^3 mol^{-1} s^{-1}]	E [kJ mol^{-1}]
$k_{\mathrm{p,\ chem}}$	$8.7 \pm 0.2 \times 10^{-1}$	24.9 ± 1.0
$k_{\mathrm{tr,\ chem}}$	$8.9 \pm 0.3 \times 10^{-4}$	54.3 ± 2.2
$k_{\mathrm{tc,\ chem}}$	$7.1 \pm 0.8 \times 10^{+4}$	0[a]
$k_{\mathrm{tCl,\ chem}}$	$7.9 \pm 3.4 \times 10^{+5}$	0[a]
$k_{\mathrm{inCl,\ chem}}$	$6.1 \pm 0.7 \times 10^{-1}$	28.4 ± 8.0

[a] Fixed.

are given in Table 7. The correlations between the errors of the responses (lower diagonal) are sufficiently low to assume the independence of the different responses. This explains the low sensitivity of the estimated values of the parameters on the choice of $\mathbf{\Sigma}$ in the objective function (Eq. (1)). From the diagonal elements of the error covariance matrix a non-biased estimate for the pure error of each response can be calculated (Eq. (2) for $k=1$). For conversion, this is a satisfactory 5% absolute error. For the moments $\bar{M}_{\mathrm{n}}$, $\bar{M}_{\mathrm{m}}$ and $\bar{M}_{\mathrm{z}}$ this is 3.6×10^3, 7.9×10^3 and 2.3×10^4 g mol^{-1} as compared to absolute values of about 5×10^4, 1×10^5 and 2×10^5, respectively.

From Table 6, it can be seen that the estimates of the Arrhenius parameters for propagation and chain transfer to

Table 7
Error variance–covariance matrix (diagonal and above diagonal) estimated with Eq. (2) and corresponding error correlation matrix (below diagonal) between the responses for monomer conversion (X) and the moments ($\bar{M}_{\mathrm{n}}$, $\bar{M}_{\mathrm{m}}$, $\bar{M}_{\mathrm{z}}$) of the molecular mass distribution

Response	X	$\bar{M}_{\mathrm{n}}$	$\bar{M}_{\mathrm{m}}$	$\bar{M}_{\mathrm{z}}$
X	2.63×10^{-3}	3.04×10^1	-1.41×10^1	-3.30×10^1
$\bar{M}_{\mathrm{n}}$	0.164	1.31×10^7	1.04×10^7	5.62×10^6
$\bar{M}_{\mathrm{m}}$	−0.035	0.366	6.17×10^7	1.15×10^8
$\bar{M}_{\mathrm{z}}$	−0.028	0.068	0.644	5.17×10^8

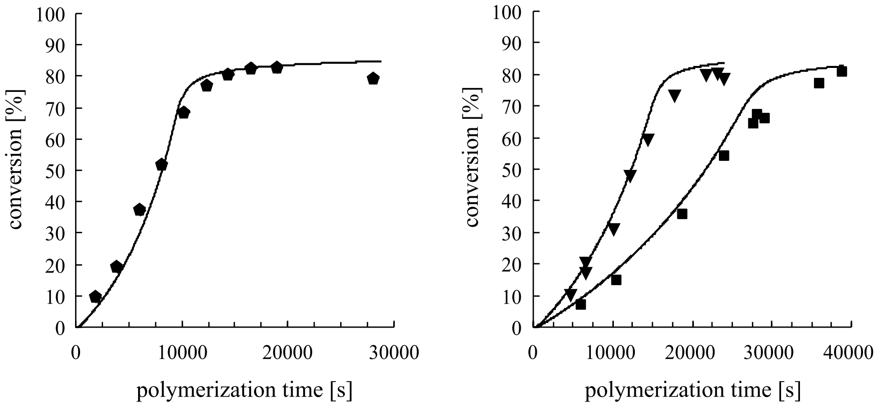

(a) 308K (b) 318K

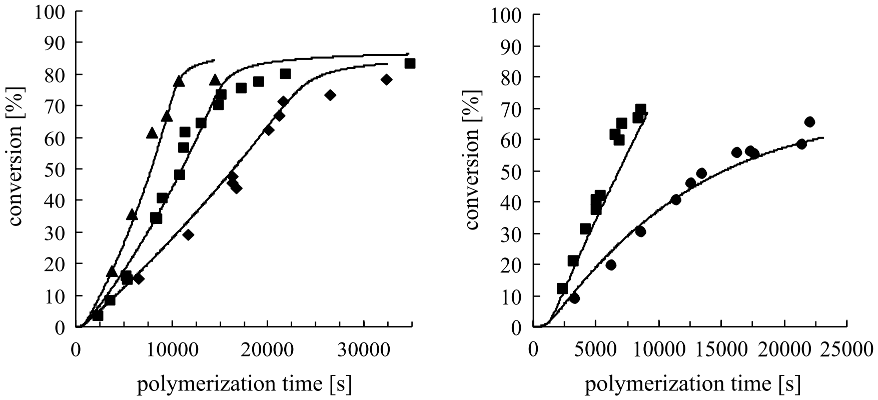

(c) 328K (d) 338K

Fig. 1. Monomer conversion as a function of polymerization time for given temperatures and concentrations of the initiator *tert*-butyl peroxyneodecanoate (TBPD). Initiator wt%: ●, 0.0262; ◆, 0.0392; ■, 0.0785; ▲, 0.1569; ▼, 0.2354; ⬟, 3.02. Solid lines are calculated using equations in Table 4 with set of intrinsic Arrhenius parameter values given in Table 6 and $k_{\mathrm{d},k} = 1.52 \times 10^{14} \exp(-115{,}470/RT)$, $f_{\mathrm{chem}} = 0.7$.

monomer are most accurate. This can be explained by the fact that the parameters corresponding to these reactions influence the calculation of the conversion and molecular mass distribution to a larger extent than the other parameters. The 95% confidence interval of the Arrhenius parameters related to the chain initiation reaction by a Cl radical is wider in comparison to the 95% confidence interval of the other parameters. The value of the $k_{\mathrm{inCl,chem}}$ rate coefficient is only affecting the calculation of the monomer conversion and not the calculation of the moments of the molecular mass distribution (Tables 4 and 5). Therefore, less experimental data are available to estimate the Arrhenius parameters corresponding to this reaction in comparison to the other parameters, resulting in a less accurate estimate.

The estimated activation energies of propagation and chain transfer to monomer, 24.9 and 54.3 kJ mol^{-1}, respectively, correspond well with earlier reported values of 27.6 and 50.6 kJ mol^{-1} [8]. For the Arrhenius parameters corresponding to the other reactions no literature values are available. Differences between the values of rate coefficients at a given temperature reported in this article and previously reported values can be explained by the different treatment of diffusion limitations. Indeed, the applied diffusion model always has an influence on the estimated intrinsic rate coefficients. The accuracy of the obtained values for these intrinsic parameters, however, increases when diffusion effects are accounted for independently.

A comparison between the calculated and experimental conversion and moments of the MMD as a function of polymerization time is shown in Figs. 1 and 2. A good agreement is observed.

The F value for the significance of the regression amounts to 3538. The binary correlation coefficients between the parameter estimates shown in Table 8 are lower than 0.9, signifying a sufficiently low correlation.

The calculated moments $\bar{M}_{\mathrm{n}}$ and $\bar{M}_{\mathrm{m}}$ of the MMD correspond well with experimental data over the complete range of investigated conditions, while the calculated $\bar{M}_{\mathrm{z}}$ is too low up to intermediate polymerization times (Fig. 2). After a short initial rise of the calculated molecular mass in the first stage of the polymerization, the heating of the reactor causes the calculated moments to decrease at the start of the polymerization. However, the latter cannot entirely explain the difference between the observed and the calculated $\bar{M}_{\mathrm{z}}$ profile. The deviation between the simulated and experimental $\bar{M}_{\mathrm{z}}$ can be attributed to the transfer of macroradicals between the monomer-rich phase and the polymer-rich phase. In the present model, it is assumed that macroradicals do not transfer between phases: Only the transfer of dead polymer molecules from the monomer-rich phase to the polymer-rich phase is taken into account. As the apparent termination rate coefficient in the polymer-rich phase is lower then in the monomer-rich phase, because of the gel effect, taking into account the transfer of macroradicals from the monomer rich phase to the polymer-rich phase would produce longer chains, which could explain the deviations for $\bar{M}_{\mathrm{z}}$ as seen in Fig. 2. At 308 K (Fig. 2(a)) the deviation is most pronounced because at this temperature the largest difference is calculated between the average molecular mass produced in the monomer-rich phase and in the polymer-rich phase. This

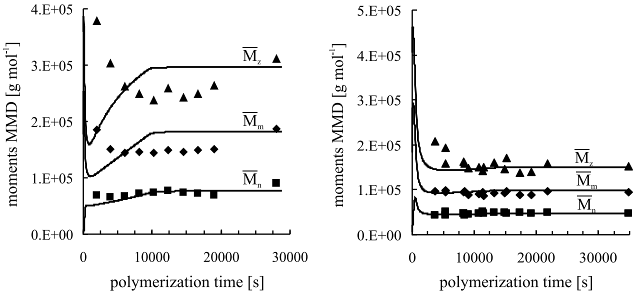

(a) 308K, 3.02wt%

(b) 328K, 0.0785wt%

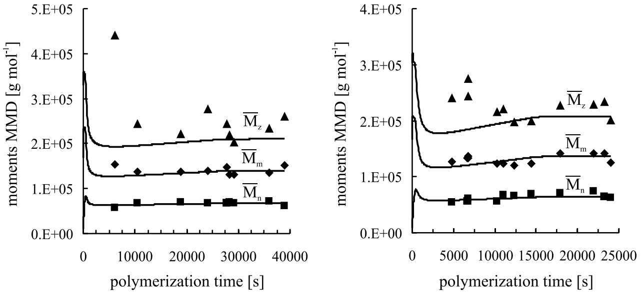

(c) 318K, 0.0785wt%

(d) 318K, 0.2354wt%

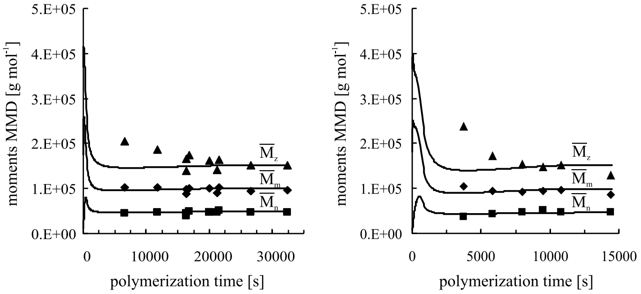

(e) 328K, 0.0392wt%

(f) 328K, 0.1569wt%

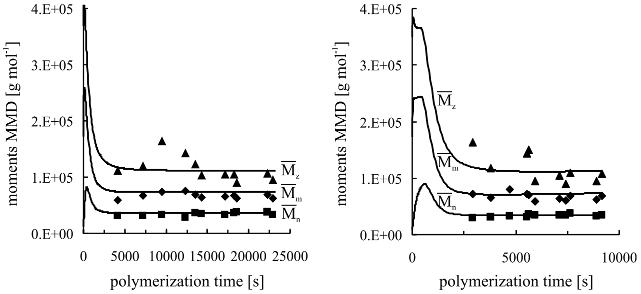

(g) 338K, 0.0262wt%

(h) 338K, 0.0785wt%

Fig. 2. Moments of the molecular mass distribution (experimental: ■, $\bar{M}_{\mathrm{n}}$; ◆, $\bar{M}_{\mathrm{m}}$; ▲, $\bar{M}_{\mathrm{z}}$) as a function of polymerization time for given temperatures and concentrations of the initiator *tert*-butyl peroxyneodecanoate (TBPD). Solid lines are calculated using equations in Table 5 with the set of intrinsic Arrhenius parameter values given in Table 6 and $k_{\mathrm{d},k} = 1.52\times10^{14}\exp(-115{,}470/RT)$, $f_{\mathrm{chem}} = 0.7$.

Table 8
Binary correlation matrix between the estimates of the reparameterized pre-exponential factor and activation energy of the intrinsic rate coefficients for propagation, $k_{\mathrm{p,chem}}$, for chain transfer to monomer, $k_{\mathrm{tr,chem}}$, for termination, $k_{\mathrm{tc,chem}}$ and $k_{\mathrm{tCl,chem}}$, and for chain initiation by a Cl radical, $k_{\mathrm{inCl,chem}}$

		$k_{\mathrm{p,\ chem}}$		$k_{\mathrm{tr,\ chem}}$		$k_{\mathrm{tc,\ chem}}$	$k_{\mathrm{tCl,\ chem}}$	$k_{\mathrm{inCl,\ chem}}$	
		A^*	E	A^*	E			A^*	E
$k_{\mathrm{p,\ chem}}$	A^*	1.0							
	E	−0.393	1.0						
$k_{\mathrm{tr,\ chem}}$	A^*	0.657	−0.353	1.0					
	E	−0.496	0.569	−0.7476	1.0				
$k_{\mathrm{tc,\ chem}}$		0.826	0.117	0.394	−0.029	1.0			
$k_{\mathrm{tCl,\ chem}}$		0.213	−0.754	0.252	−0.627	−0.571	1.0		
$k_{\mathrm{inCl,\ chem}}$	A^*	−0.405	−0.287	−0.311	0.120	0.503	0.374	1.0	
	E	0.128	−0.865	0.183	−0.327	−0.160	0.821	0.418	1.0

is caused by the smaller chain transfer to monomer rate coefficient $k_{\mathrm{tr},k}$ (highest activation energy) giving a MMD in each phase much more determined by termination than at higher temperatures. Therefore, at low polymerization times shorter chain lengths are calculated because in the applied model most of the polymer is produced in the monomer-rich phase. At higher polymerization times the polymer chain length increases because most of the polymer is produced in the polymer-rich phase, in which longer chains are formed. It is expected that adding the transfer of macroradicals between the monomer-rich and the polymer-rich phase to the model will hardly affect the estimated values for the intrinsic rate coefficients because the influence is only pronounced at low conversions and for one of the three moment responses, namely $\bar{M}_{\mathrm{z}}$.

6.2. Effect of diffusion on termination reactions

The chain length dependency of the apparent termination by combination rate coefficient, $k_{\mathrm{tc}}^{i,j}$, is shown in Fig. 3(a). This behavior is a consequence of the chain length dependency of the diffusion coefficient $D_{\mathrm{p+rd}}^{i}$ of the macroradicals $R_{i,2}$. From Fig. 3(b), it can be seen that $D_{\mathrm{p+rd}}^{i}$ decreases rapidly as a function of chain length. Until a chain length of $i \approx 2000$, $D_{\mathrm{p+rd}}^{i}$ decreases; then it reaches a plateau at a value of $\pm 3\times10^{-18}$ m^2 s^{-1}. This is due to the two diffusion coefficient contributions of the diffusion coefficient $D_{\mathrm{p+rd}}^{i}$: D_{p}^{i} calculated with the free volume theory and the reaction diffusion coefficient D_{rd}. At a chain length of $i \approx 2000$, D_{p}^{i} becomes so small that for higher chain lengths the reaction diffusion is the dominant diffusion coefficient contribution in $D_{\mathrm{p+rd}}^{i}$. From Fig. 3(a) it can be seen that the reaction of a macroradical with chain length $j=1$ is only weakly diffusion-controlled, since $k_{\mathrm{tc},2}^{i,1}$ is independent of i. The termination rate coefficient for macroradicals $R_{j,2}$ with higher chain lengths, $k_{\mathrm{tc},2}^{i,j}$ decreases very fast as a function of i and reaches an asymptotic value which is determined by the diffusion coefficient of the smallest macroradical. For example, with $j=10$, the asymptotic value of $k_{\mathrm{tc},2}^{i,10}$ is already one order of magnitude lower than that of $k_{\mathrm{tc},2}^{i,1}$.

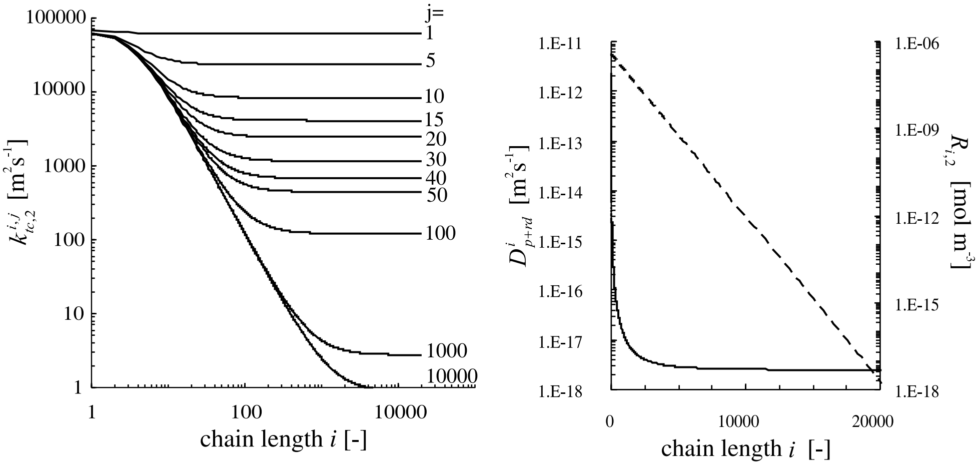

(a) $K_{tc,2}^{i,j}$

(b) D_{p+rd}^{i} and $R_{i,2}$

Fig. 3. (a) Apparent termination by combination rate coefficient $k_{\mathrm{tc},2}^{i,j}$ between macroradicals $R_{i,2}$ and $R_{j,2}$ in the polymer-rich phase as function of the chain lengths i and j (from Eqs. (4) and (16)); the profiles for $j=10{,}000$ and $j=20{,}000$ are indistinguishable. Reaction conditions: 328 K, 0.0785 wt% initiator *tert*-butyl peroxyneodecanoate ($k_{\mathrm{d},2}=1.52\times10^{14}\exp(-115{,}470/RT)$, $f_{\mathrm{chem}}=0.7$), $t=1630$ s, conversion = 3.3%. $\langle k_{\mathrm{tc},2}\rangle=945$ m^3 mol^{-1} s^{-1}, $\omega_{\mathrm{p}}=0.70$. (b) (solid line) Macroradical diffusion coefficient $D_{\mathrm{p+rd}}^{i}$ from Eq. (12) and (dotted line) macroradical concentration in the polymer-rich phase $R_{i,2}$ as a function of the chain length i, from applying pseudo-steady-state approximation to $R_{i,2}$ using equations from Table 4.

The macroradical concentrations $R_{i,2}$ decrease as a function of chain length i, as is shown in Fig. 3(b). The $R_{i,2}$ are calculated using a coarse graining technique to solve the equations obtained by applying the pseudo-steady-state approximation to the $R_{i,2}$ balances from Table 4. As mentioned before, this coarse graining technique divides the macroradical distribution into several classes, assuming that the concentration of the radicals within a class Δ_I is equal to a constant value $R_{I',2}$. The $R_{I',2}$ are obtained from $R_{I,2}$ via Eq. (32). The latter are determined by the $R_{\mathrm{I}-1,2}$ multiplied with a propagation probability, which is close to one during the polymerization process (Eq. (36)). As a result, a straight line as a function of chain length is observed. As the termination between two macroradicals $R_{i,k}$ and $R_{j,k}$ occurs via combination, the termination between a Cl_k radical and a macroradical $R_{i,k}$ is also assumed to occur via combination. The estimated value for $k_{\mathrm{tCl,chem}}$ (Table 6) is one order of magnitude larger than $k_{\mathrm{tc,chem}}$ and is situated in between the values for bimolecular termination between macroradicals and bimolecular termination between halogenic radicals, such as Cl [45]. Note, however, that the concentration of macroradicals is typically three orders of magnitude higher than that of the Cl radicals. Hence, in the monomer-rich phase the intrinsic termination rate corresponding to recombination of macroradicals is still two orders of magnitude higher. In the polymer-rich phase, accounting for the higher diffusion rate of Cl radicals compared with macroradicals, however, the apparent termination rate by recombination of macroradicals is only one order of magnitude higher, as long as there is a monomer-rich phase. As soon as the latter disappears, the polymer concentration in the polymer-rich phase starts to increase. Hence, the diffusion limitations become more pronounced, in particular for the recombination of two macroradicals. Termination by Cl radicals attenuates strongly this gel effect. The importance of termination with Cl radicals is illustrated in Fig. 4. The calculated monomer conversion and polymer-rich phase termination rate with and without Cl radical termination are compared as a function of batch time. Accounting for Cl radical termination decreases the final conversion with 10% and provides agreement with the measured conversion, see Fig. 1.

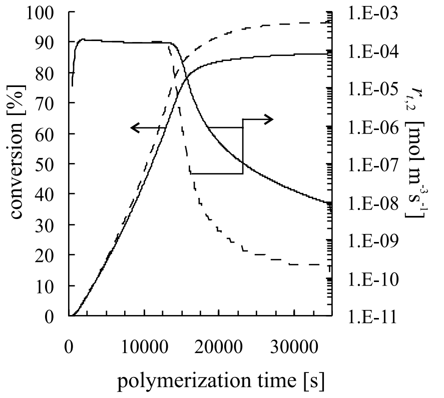

Fig. 4. Calculated monomer conversion (328 K, 0.0785 wt% initiator) and polymer-rich phase termination rate $r_{t,2}$ as a function of polymerization time (from equations in Table 4, parameter values taken from Table 6). Solid line: Calculations including Cl radical termination, $r_{t,2}=\langle k_{tc,2}\rangle\left(\sum_i R_{i,2}\right)^2+k_{tCl,2}\mathrm{Cl}_2\sum_i R_{i,2}$; dotted line: Calculations excluding Cl radical termination, $r_{t,2}=\langle k_{tc,2}\rangle\left(\sum_i R_{i,2}\right)^2$.

7. Conclusions

The Arrhenius parameters of the intrinsic rate coefficients for propagation, $k_{\mathrm{p,chem}}$, for chain transfer to monomer, $k_{\mathrm{tr,chem}}$, for chain initiation by a Cl radical, $k_{\mathrm{inCl,chem}}$, and for termination by combination, $k_{\mathrm{tc,chem}}$ and $k_{\mathrm{tCl,chem}}$, in the vinyl chloride suspension polymerization are estimated. The diffusion contributions in the apparent rate coefficients are calculated from the physical properties of the reaction medium. Termination by combination between two macroradicals is dominant over the termination by disproportionation between macroradicals. Termination of macroradicals with Cl radicals has to be taken into account because it decreases the final conversion in the third stage of the polymerization by the attenuation of the gel effect. The estimated intrinsic rate coefficients allow to obtain a good agreement between experimental and calculated conversion and moments of the molecular mass distribution ($\bar{M}_{\mathrm{n}}, \bar{M}_{\mathrm{m}}, \bar{M}_{z}$) as a function of polymerization time for a broad range of temperatures and initiator concentrations as well as of conversion. However, comparison of calculated and experimental values for the moments of the MMD suggests that transfer of macroradicals between the monomer-rich phase and the polymer-rich phase can significantly affect the $\bar{M}_{z}$ molecular mass profile at low conversions. Explicitly and independently accounting for the diffusional transport next to the intrinsic reaction kinetics is necessary in order to construct kinetic models for polymerization reactions which are valid over a wide range of conditions.

Acknowledgements

BASF Antwerp and SolVin are acknowledged for financial support and permission to publish this work. This research has been done as a part of the Interuniversity Attraction Poles Programme funded by the Belgian Science Policy. J. Wieme is grateful to the Fund for Scientific Research-Flanders (F.W.O.-Vlaanderen) for a Research Assistantship.

References

[1] Xie TY, Hamielec AE, Wood PE, Woods DR. Polymer 1991;32(11): 2087–95.

[2] Xie TY, Hamielec AE, Wood PE, Woods DR. J Vinyl Tech 1991; 13(1):2–25.

[3] Kiparissides C, Daskalakis G, Achilias DS, Sidiropoulou E. Ind Eng Chem Res 1997;36:1253–67.

[4] Talamini G, Visentini A, Kerr J. Polymer 1998;39(10):1879–91.

[5] Talamini G, Kerr J, Visentini A. Polymer 1998;39(18):4379–84.

[6] Krallis A, Kotoulas C, Papadopoulos S, Kiparissides C, Bousquet J, Bonardi C. Ind Eng Chem Res 2004;43:6382–99.

[7] Burnett GM, Wright WW. Proc R Soc A 1954;221:37–41.

[8] Abdel-Alim AH, Hamielec AE. J Appl Polym Sci 1972;16(3):783–99.

[9] van Herk AM. Macromol Theory Simul 2000;9(8):433–41.

[10] Beuermann S. Macromol Symp 2002;182:31–42.

[11] Habibi A, Vasheghani-Farahani E. AIChE J 2004;50(6):1260–72.

[12] Dubé MA, Soares JBP, Penlidis A, Hamielec AE. Ind Eng Chem Res 1997;36:966–1015.

[13] Goodner MD, Lee HR, Bowman CN. Ind Eng Chem Res 1997;36: 1247–52.

[14] Tefera N, Weickert G, Westerterp KR. J Appl Polym Sci 1997;63(12): 1649–61.

[15] Tefera N, Weickert G, Westerterp KR. J Appl Polym Sci 1997;63(12): 1663–80.

[16] De Roo T, Heynderickx GJ, Marin GB. Macromol Symp 2004;206(1): 215–28.

[17] Burgess RH. Manufacture and processing of PVC. London: Applied Science Publishers Ltd; 1982.

[18] Froment GF, Hosten LH. In: Anderson J, Boudart M, editors. Catalysis—science and technology, vol. 2. Berlin: Springer; 1981. p. 97–170.

[19] Boggs PT, Byrd RH, Rogers JE, Schnabel RB. National Institute of Standards and Technology, Gaithersburg; 1992.

[20] Gilbert RG. Pure Appl Chem 1992;64(10):1563–7.

[21] de Kock JBL, van Herk AM, German AL. J Macromol Sci Polym Rev 2001;C41(3):199–252.

[22] Smoluchowski M. Z Phys Chem 1917;92:129–68.

[23] Buback M, Sandmann J. Z Phys Chem 2000;214(5):583–607.

[24] Russell GT, Gilbert RG, Napper DH. Macromolecules 1992;25: 2459–69.

[25] Russell GT, Gilbert RG, Napper DH. Macromolecules 1993;26: 3538–52.

[26] Zielinski JM, Duda JL. AIChE J 1992;38(3):405–15.

[27] Zielinski JM. Macromolecules 1996;29(18):1098–111.

[28] Vrentas JS, Vrentas CM. Eur Polym J 1998;34(5/6):797–803.

[29] Neogi P. Diffusion in polymers. 1st ed. New York: Marcel Dekker; 1996.

[30] Dullien FAL. AIChE J 1972;18(1):62–70.

[31] Daupert TE, Danner RP. Data compilation tables of properties of pure compounds. New York: Design Institute of Physical Property Data (DIPPR), American Institute of Chemical Engineers (AIChE); 1985.

[32] Perry RH, Green DW. Perry's chemical engineers' handbook. 7th ed.: New York: McGraw-Hill International Editions; 1997.

[33] Mark JE. Physical properties of polymers handbook. Woodbury, New York: AIP Press; 1996.

[34] Gallant RW. Hydrocarbon processing 1966;45(6):153–60.

[35] Van Krevelen DW. Properties of polymers—their correlation with chemical structure; their numerical estimation and prediction from additive group contributions. 3rd ed. Amsterdam: Elsevier; 1997.

[36] Ferry JD. Viscoelastic properties of polymers. 2nd ed. New York: Wiley; 1970.

[37] Brandrup J, Immergut EH. Polymer handbook. 3rd ed. New York: Wiley; 1989.

[38] Doi M, Edwards SF. The theory of polymer dynamics. Oxford: Oxford University Press; 1986.

[39] Masaro L, Zhu XX. Prog Polym Sci 1999;24(5):731–75.

[40] Graessley WW. J Polym Sci Polym Phys 1980;18(1):27–34.

[41] Graessley WW. J Polym Sci Polym Phys 1996;34(16):2663–4.

[42] Aharoni SM. Macromolecules 1986;19:426–34.

[43] Tonge MP, Gilbert RG. Polymer 2001;42(2):501–13.

[44] Monteiro MJ, Subramaniam N, Taylor JR, Pham BTT, Tonge MP, Gilbert RG. Polymer 2001;42:2403–11.

[45] Ingold UI. In: Kochi JK, editor. Free radicals, vol. 1. New York: Wiley; 1973. p. 37–112.